

# High dispersion spectroscopy of two A supergiant systems in the Small Magellanic Cloud with novel properties

R.E. Mennickent,<sup>1\*</sup> M. A. Smith<sup>2</sup>

<sup>1</sup>*Universidad de Concepción, Departamento de Astronomía, Casilla 160-C, Concepción, Chile*

<sup>2</sup>*Department of Physics, Catholic University of America, Washington, DC 20064, USA; Present address: Space Telescope Science Institute, 3700 San Martin Dr., Baltimore, MD 21218, USA*

## ABSTRACT

We present the results of a spectroscopic investigation of two novel variable bright blue stars in the SMC, OGLE004336.91-732637.7 (SMC-SC3) and the periodically occulted star OGLE004633.76-731204.3 (SMC-SC4), whose photometric properties were reported by Mennickent et al. (2010). High-resolution spectra in the optical and far-UV show that both objects are actually A + B type binaries. Three spectra of SMC-SC4 show radial velocity variations, consistent with the photometric period of 184.26 days found in Mennickent et al. 2010. The optical spectra of the metallic lines in both systems show combined absorption and emission components that imply that they are formed in a flattened envelope. A comparison of the radial velocity variations in SMC-SC4 and the separation of the  $V$  and  $R$  emission components in the  $H_\alpha$  emission profile indicate that this envelope, and probably also the envelope around SMC-SC3, is a *circumbinary* disk with a characteristic orbital radius some three times the radius of the binary system. The optical spectra of SMC-SC3 and SMC-SC4 show, respectively, He I emission lines and discrete Blue Absorption Components (“BACs”) in metallic lines. The high excitations of the He I lines in the SMC-SC3 spectrum and the complicated variations of Fe II emission and absorption components with orbital phase in the spectrum of SMC-SC4 suggests that shocks occur between the winds and various static regions of the stars’ co-rotating binary-disk complexes. We suggest that BACs arise from wind shocks from the A star impacting the circumbinary disk and a stream of former wind-efflux from the B star accreting onto the A star. The latter picture is broadly similar to mass transfer occurring in the more evolved (but less massive) Algol (B/A + K) systems, except that we envision transfer occurring in the other direction and not through the inner

Lagrangian point. Accordingly, we dub these objects prototype of a small group of Magellanic Cloud wind-interacting A + B binaries.

**Key words:** stars: early-type, stars: evolution, stars: mass-loss, stars: Ae stars: variables-others

## 1 INTRODUCTION

Mennickent et al. (2002, hereafter M02) have reported the existence of a number of bright blue stars in the Small Magellanic Cloud the light curves of which exhibit periodic or quasi-periodic variability in their OGLE (Udalski et al. 1997) *I*-band light curves. In an initial follow up of the investigation, Mennickent et al. (2006; “M06”) noted that some stars exhibit peculiar spectroscopic properties and multiple periods. They gave initial estimates of spectral classifications based on low dispersion spectra, but they noted conflicting properties. In a companion study to this one, Mennickent et al. (2010; hereafter “M10”) have selected two novel Type 3 variables<sup>1</sup> with novel properties named OGLE004336.91-732637.7 ( $\equiv$  SMC-SC3-63371, MACHO ID 213.15560; hereafter SMC-SC3) and OGLE004633.76-731204.3 ( $\equiv$  SMC-SC4-67145, MACHO ID 212.15735.6; hereafter SMC-SC4). These Type 3 stars were chosen according to the sole additional arbitrary criterion that they are brighter than  $m_v = 14.2$ . The photometric analysis in M10 was based on new OGLE III light curves and found that SMC-SC3 exhibits a double-minimum period with a period of 238.1 days and a second quasi-period that fluctuates between two values each near 15.35 days. The appearance of the longer period, which exhibits minima at unequal spacings and unequal depths suggests the appearance of an ellipsoidal variable. The high orbital eccentricity implied by these properties is confirmed by the inference from the sharp and unequal light maxima that reflection effects from a secondary occur during brief periastron passages. The light curve of SMC-SC4 reveals surprising periodic deep eclipses every 184.26 days, modulated over a superperiod of several cycles, and chaotic variability indicative of multiple shorter periods.

M06 and M10 have open a variety of questions that can be pursued with high resolution spectra, which we undertake to pursue now. We have already remarked as one example that the spectra of SMC-SC3 and SMC-SC4 spectra are unusual in that they show properties of rather conflicting spectral types (strong Na D and strong  $H_\alpha$  and  $H_\beta$  emission components). Therefore, we obtained three high-dispersion optical spectra of SMC-SC3 and SMC-SC4 during the period 2002-9. To

\* E-mail: rmennick@astro-udec.cl. Based on observations carried out at ESO telescopes: ESO proposal 69.D-0391(A), backup targets.

<sup>1</sup> Mennickent Type-3 variables are SMC Be star candidates with *I*-band light curves varying periodically or quasi-periodically.

**Table 1.** Summary of observations. The MJD numbers at mid exposure are given. The periods detected in photometric data are also given. Phases refer to the ephemeris given in Mennickent et al. (2010). CD refers to cross-disperser.

object	periods (d)	instrument	UT-date	airmass	$\Delta\lambda$ (Å)	grating	exptime (s)	mjd-obs	phase	S/N
SMC-SC3	238, 15	UVES	2002/05/17	1.96	3100–8500	CD#1,3	600	52411.39633	0.28	25
SMC-SC3		UVES	2002/05/17	1.91	3100–10400	CD#1,4	600	52411.40536	0.28	20
SMC-SC4	184	UVES	2002/05/17	1.86	3100–8500	CD#1,3	600	52411.41614	0.23	20
SMC-SC4		UVES	2002/05/17	1.81	3100–10400	CD#1,4	600	52411.42782	0.23	15
SMC-SC3		MIKE	2007/11/09	1.43	3390–9410	echelle	500	54413.03654	0.69	25
SMC-SC4		MIKE	2007/11/09	1.42	3390–9410	echelle	500	54413.04421	0.10	40
SMC-SC3		Echelle	2009/08/25	1.44	3940–7490	echelle	2000	55068.24680	0.44	17
SMC-SC4		Echelle	2009/08/25	1.40	3940–7490	echelle	2000	55068.27751	0.66	17

**Table 2.** Summary of *FUSE* Observations. Phases refer to the ephemeris given in Mennickent et al. (2010).

object	UT-date	UT-start	exptime (s)	mjd-obs	phase
SMC-SC3	2006/10/05	04:05:06	2430	54013.18427083	0.01
SMC-SC4	2006/11/30	11:36:26	2736	54069.49946759	0.24

obtain a better understanding of how the spectra appear at short wavelengths we obtained a *Far Ultraviolet Spectroscopic Explorer (FUSE)* spectrum of both stars. These spectra and the *FUSE* data form the basis of this investigation. The goal of our study is to elucidate the properties of the circumstellar environment of these objects and to pave the way to understanding the evolutionary state of this potential new subclass of Ae stars.

## 2 OBSERVATIONS AND DATA REDUCTION

High resolution spectra were obtained on 2002 May 17 with the ESO Ultraviolet-Visual Echelle Spectrograph in dichroic modes at the UT 2 telescope in the ESO Paranal Observatory, Chile. The three CCD chips on this instrument allowed sampling the spectral range of 3100–10400 Å. A slit width of 1'' allowed us to obtain spectra at resolving power  $\sim 40\,000$ . The spectra were normalized to the continuum, and no flux calibration or telluric correction was needed. Additional spectra were obtained with the *Magellan Inamori Kyocera Echelle (MIKE)* spectrograph at the Clay Telescope in Las Campanas Observatory, Chile on 2007 November 9. This double echelle spectrograph provided wavelength coverage of 3390–4965 Å (blue camera) and 4974–9407 Å (red camera). With a slit width of 0.7'' the resolving power was again 40 000. The spectra were reduced and calibrated with IRAF. We obtained a third spectrum for each star on 2009 August 25 with the echelle spectrograph mounted in the 2.5m DuPont telescope of Las Campanas Observatory, Chile; this is referred to as the “LCO” spectrum in our figure captions. The wavelength range in this case was 3940–7490 Å and the resolving power again of 40 000. These spectra were also reduced and calibrated with standard IRAF routines.

A summary of the optical spectroscopic observations is given in Table 1. The spectra of SMC-SC4

were obtained at phases 0.23, 0.10, and 0.66, respectively, in the 184.26 day period identified in M10. The zeropoint is taken as the mid-eclipse in the light curves, i.e., at the light minima. For SMC-SC3 the spectra were taken at phases 0.28, 0.69, and 0.44, according to the 238.1 day period identified in M10.

In addition, far-UV spectra of SMC-SC3 and SMC-SC4 were obtained through the large science aperture of the *Far Ultraviolet Spectroscopic Explorer (FUSE)* in 2006 October-November under GO Cycle 6 Program F907, as detailed in Table 2. A spectrum of OGLE005100.18-725303.0 was obtained on 2006 October 6, as a quasi-standard. The *FUSE* spectra cover the continuous wavelength range 929-1188 Å over eight MAMA detector segments. The *FUSE* spectrum is recorded on two of these segments, thereby insuring the acquisition of two independent and simultaneous spectra. The spectral resolving power among these varies with wavelength but is typically in the range 15 000-20 000. These spectra were reduced with the CalFUSE version 3.1.8 pipeline system, which was similar to version, v3.2, which was used for the final reprocessing of the *FUSE* archive. Examination of auxiliary files that display the positions of photon events on the detector in the spatial direction confirm that they originate from an effective point source. This fact effectively rules out that the ultraviolet fluxes are contaminated by a nearby comparably bright source in the science aperture.

### 3 RESULTS

The optical spectra of the two program stars are complicated, and it is therefore helpful to describe their general properties before carrying out a quantitative analysis of their spectral features. These spectra are redshifted by amounts of roughly 2 Å, which is typical for optical spectra of members of the SMC.

#### 3.1 Reconnaissance of the optical spectra

In many respects the optical spectra are similar to the spectrum of a typical A supergiant. This statement is demonstrated in Figure 1, which shows the high-level Balmer lines and the blue-green UVES spectra of SMC-SC3 and SMC-SC4 and of the Galactic A5 II star HD 74252 from the UVES atlas (Bagnulo et al. 2003). The cores of the hydrogen and metallic lines in the spectra of the program stars are influenced by two competing effects. On one hand, the strengths of the metallic lines are weakened in our objects due to their low metallicities. This effect is largely compensated by the presence of a substantial disk contribution, the details of which we present below.

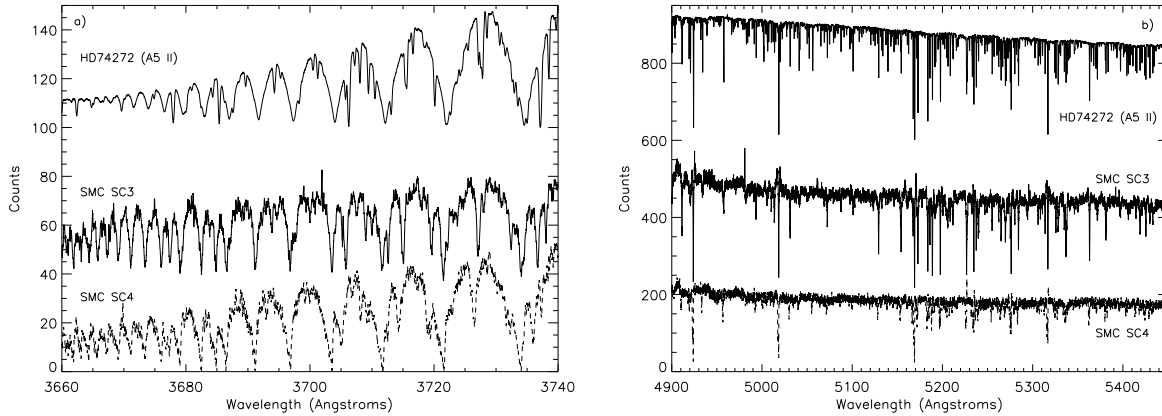


**Figure 1.** The optical UVES spectrum of the target stars and the Galactic A5II standard HD 74252 taken from the UVES atlas covering (left panel) the high level Balmer lines and (right panel) the metallic lines in the region 4900-5450 Å. The standard and SMC-SC3 have been offset in flux for convenience, and SMC-SC3 and SMC-SC4 have been blueshifted to the rest frame. The general appearance of the metallic lines shown for the two SC targets is similar to that of the standard’s lines. The Fe II lines 4923 Å 5018 Å 5176 Å and 5316 Å, are discussed in the text. Careful inspection shows that the wings of these particular lines show emission in SMC-SC3.

The cores of both hydrogen and metallic lines are stronger in SMC-SC3 than in SMC-SC4. Detailed inspection shows that most of these lines arise from once-ionized Fe-like ions and of mixed stages of light metals (Mg I, Si II, Ti II, Ca I), and these will be discussed in §3.5-3.7. Thus, the correspondence is good between the optical spectra of our stars and a middle-A, class I-II supergiant. As noted in M10, an A supergiant spectral type is also inferred from the colors and magnitudes of these objects. The spectral types will be refined in our discussion of the Ca II line profile (§3.2).

However, in other respects there are stark contrasts between the spectra of our program stars and A supergiants. We have already pointed out some of the strongest lines in our optical spectra, such as the Na I doublet, (Figure 2) and the strong  $H_\alpha$  emission. In contrast to the merely faint Beals Type I P Cygni emission, e.g., in the Bagnulo et al. (2003) spectrum of the A6 Ia standard HD 97534 the  $H_\alpha$  profiles are not only strong but double peaked with nearly equal “V” and “R” emission components - see Figure 3. The strengths of these components are shown in Table 3. These  $H_\alpha$  profiles also resemble those of Be stars at the high end of their distribution of  $H_\alpha$  strengths, although they are not quite extraordinary among Be stars. These attributes indicate the presence of a flattened, Keplerian disk. In contrast to the SMC-SC4 profiles, the  $H_\alpha$  emission of SMC-SC3 decreased over time, suggesting that these changes were monotonic over time and not due to stellar or binary activity.

The optical spectrum of SMC-SC3 is likewise well populated with sharp lines of light and Fe-group elements. The Fe II lines, those arising from levels at 2.9 eV are particularly prominent. All of these are characteristic of the spectrum of a Be star disk seen at high inclination. In a few cases discussed below weak symmetric emissions are superposed on some of the strongest Fe II lines

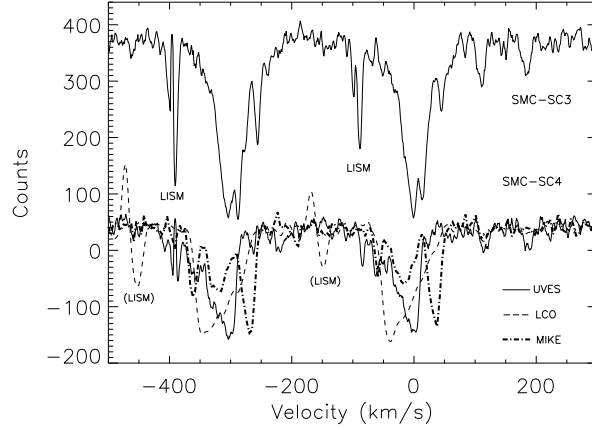


**Figure 2.** A comparison of the Na I D doublet lines in our UVES spectra, smoothed over 4 points. These systems are placed together to show the relatively symmetric profiles for SMC-SC3 and the great variations for the profiles of SMC-SC4. In the latter star the blue/red wings appear depressed in the 2002 and 2009 spectra, respectively, but the MIKE 2007 spectra shows that these shadings are caused by blendings of BAC subcomponents of widely varying relative strengths. The zeropoints of the velocity system are referred to the rest frames of the D2 (5896 Å), and in so doing the various radial velocities of the primary star have been removed. The counts for the SMC-SC4 spectra have been displaced downward by 150 units for convenience. The emission features in the LCO spectra of SMC-SC4 are telluric D line emission.

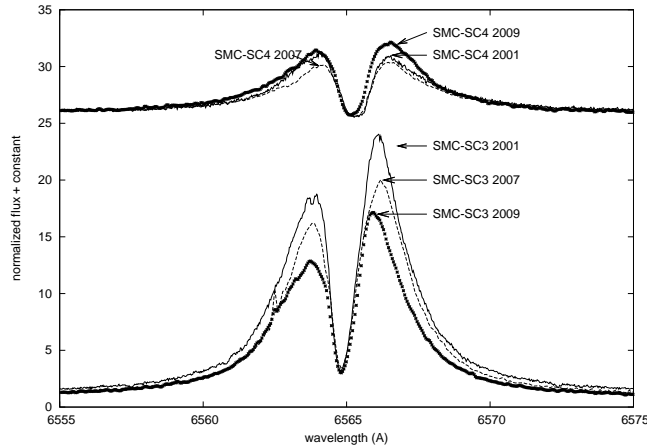


**Figure 3.** The UVES (2002), MIKE (2007) and LCO (2009) spectra depicting the  $H_\alpha$  profile for both the program stars. Fluxes are normalized to a unit continuum level (with an offset of -25 for SMC-SC4), and heliocentric corrections have been applied.

in the optical spectrum. However, unlike the spectra of B[e] stars, lines arising from metastable levels are not present, nor are [Fe] emission lines. Since these are a defining traits of B[e] stars, this star cannot be a B[e] (or “A[e]”) star.

In general the fitting of disk components to the metallic lines can be performed to compute rough column densities by assuming a local disk temperature. The spectrum of SMC-SC4 differs from the case of SMC-SC3, and for that matter from the spectrum of nearly all other known A

**Table 3.** Equivalent widths ( $EW$ ), maximum intensity relative to the continuum ( $I/I_c$ ) and full width at half maximum ( $FWHM$ ) for the  $H_\alpha$  emission line in 2002, 2007, and 2009.

Object	$-EW$ (Å)	$I/I_c$	$FWHM$ (Å)
SMC-SC3	112-104-72	24.1-22.7-17.1	4.39-4.46-4.41
SMC-SC4	28-26-33	6.3-5.7-7.1	5.16-5.25-5.02

or B stars, by the additional presence of a system of blueshifted components for most metallic lines in the optical spectrum. These discrete Blueshifted Absorption Components, which we will refer to as “BACs,” are displaced by about  $-50 \text{ km s}^{-1}$  from what we will call the main (or red) sharp component, the velocities of which adhere closely to those of the hydrogen line cores in the spectrum. Among the metallic lines the BACs are generally of comparable strength and often stronger than the main components. They tend to be barely visible or absent in weak resonance lines, e.g., in the region 3820-3850 Å. In the strong Fe II lines and the Na I D doublet a secondary BAC is also present at approximately  $-100 \text{ km s}^{-1}$  relative to the main component. Section 3.7.1 will be devoted to a discussion of these novel features.

### 3.2 Spectral Types from the Ca II H/K features

Despite the comingling of photospheric and disk features in many lines of the optical spectrum, a spectral type for our stars can be determined from the Ca H or K lines (with correction for metallicity) and the wings of the hydrogen lines. The high level Balmer and Paschen lines are consistent with a middle A-type spectral type. However, these features can vary significantly among spectra of A-type standards separated in type or luminosity class. As already mentioned, the emission in the lower members also interferes with a comparison to profiles from spectral standards or synthesis models. Consequently, we found the Ca II K line to be a more reliable indicator of the positions of the stars in the HR Diagram. The wings of this line are sensitive to electron pressure and thus luminosity class. The hydrogen lines and Fe-line metal lines already guide the spectral classification to the middle A range.

Figure 4 exhibits matches we have found for the K lines of SMC-SC3 and SMC-SC4 with the spectral standards HD 97534 (A6 Ia) and HD 74272 (A5 II) from the UVES atlas, again from the UVES atlas. We have likewise fit the spectra with SYNSPEC models for  $T_{\text{eff}} = 8500 \text{ K}$  and  $\log g = 3$ . The explicit assumption we made in our fittings was that there is no measurable contribution at this wavelength from another continuum source such as a secondary star. In general, the fits are very good, except that the models predict a narrower core than is observed in SMC-SC3 or even the core of the Ia standard (Fig 4a). In addition, the blue core of both the SMC-04 and class two standard shows an apparent “emission” feature” that the model atmospheres (with no chromosphere) do not produce (Fig. 4b). Otherwise, we estimate the precision to be  $\pm 1$  spectral subtype,  $\pm 500 \text{ K}$  in  $T_{\text{eff}}$  and  $\pm 0.5$  dex in  $\log g$ . In view of this self-consistency of our fittings with the position of the stars in the HR Diagram (M10), we judge the principal features of the optical

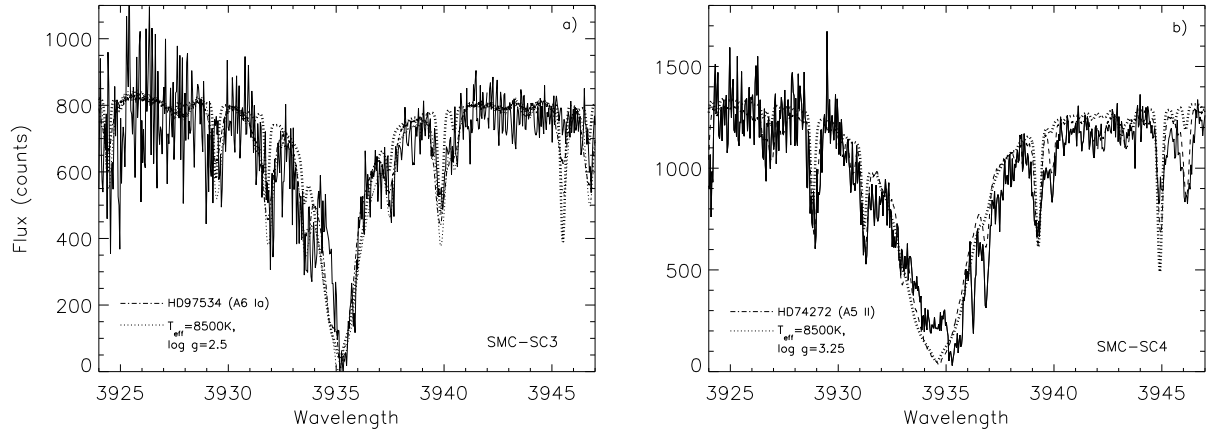


**Figure 4.** The spectral region surrounding the Ca II K line in our two program stars from our MIKE (2007) spectra. Spectra of the comparison stars HD 97534 and HD 74272 are represented by dashed lines. Fits from SYNSPEC models using Kurucz atmospheres are given by the dotted lines.

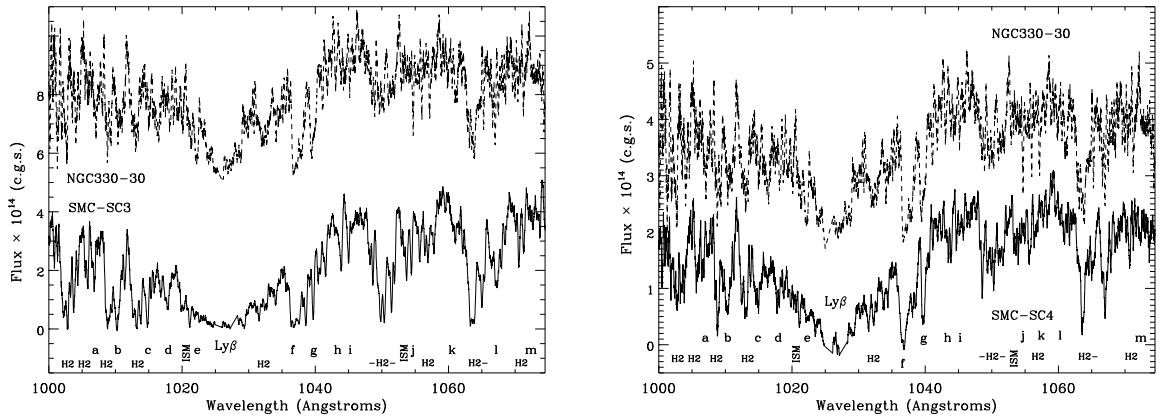


**Figure 5.** The far UV spectrum covering 1000-1070 Å for the B3 II quasi-standard of NGC 330-30 and one of our program stars, smoothed over 8 points. The spectrum of the standard is offset vertically for clarity. Several molecular H<sub>2</sub> and atomic interstellar ("ISM") lines are noted. We identify photospheric lines by coded letters. These codes have the following meaning: a) Fe III-Cr III 1007 Å, b) C II 1010.4 Å, c) Si III 1015.5 Å, d) Fe III 1018.4 Å, e) Fe III 1021.7 Å, f) C II 1036-1037 Å, g) Fe III 1039.9 Å, h) Cr III 1042.9 Å, i) Fe III 1045.2 Å, j) Mn III 1055.5 Å, k) Fe III 1058.8 Å, l) Fe III 1060.7 Å, m) Si IV 1066.6 Å, and n) Si IV-Mn III 1073 Å. The dominant Lyman β line is also indicated.

spectrum including the Ca K and hydrogen lines to be due to middle A supergiants, specifically types near A6 I and A5 II, respectively. In addition we judge that we should just be able to discern a 6% (3 magnitudes) contamination to the K line from flux of a contributing secondary.

### 3.3 Spectral types in the far-UV

Because the program *FUSE* spectra were obtained through the instrument's Large Science Aperture, we were able to estimate the far-UV flux in addition to surveying the spectral line strengths. The spectral lines are consistent with an early to mid B type spectrum and inconsistent with predictions for an A star. We concluded from this that the far-UV flux is emitted by a secondary star that is too faint to show visible lines in the optical range. Our initial reconnaissance of the hydrogen Lyman and the metallic lines suggested that the spectrum is representative of a star of type

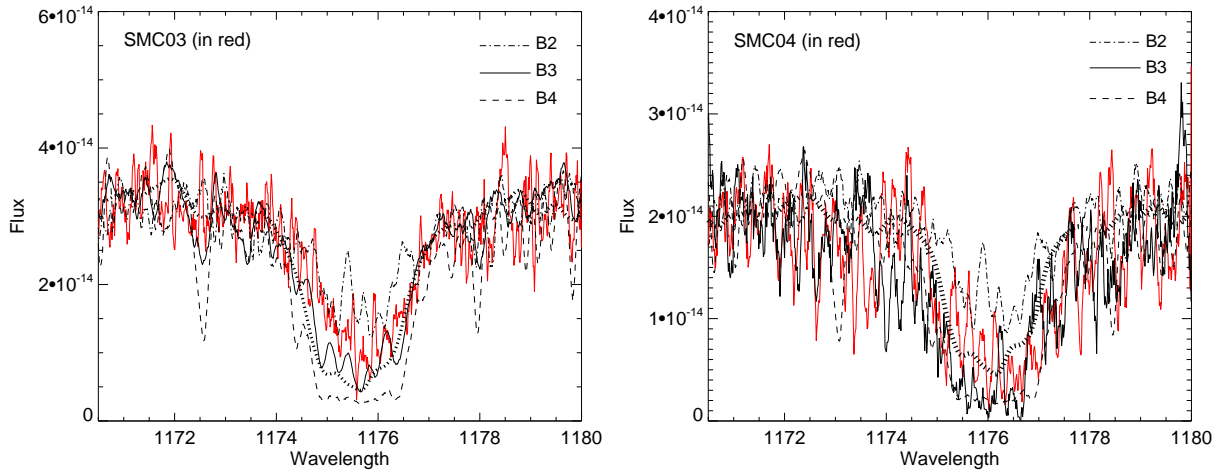


**Figure 6.** *FUSE* spectra for the region surrounding the C III 1176 Å feature in our two program stars, represented by the red line, and in three Galactic stars representing spectral types B2, B3, and B4 near the main sequence. For the panel a) these stars are HD 37367, HD 45057, and HD 201836. For panel b) we have substituted the spectrum of the B3 star NGC 330-B30 for the spectrum of HD 45057. Both B3 star spectra give much the same comparison. The dotted line is the SYNPEC spectral simulation for a  $T_{\text{eff}} = 18000\text{K}$ ,  $\log g = 3.5$ ,  $[\text{Fe}/h] = -0.7$  model.

B0 to B5. To compare our far-UV spectra with those of other metal-poor early B stars fainter than supergiants, we canvassed the entire *FUSE* archive. We found only four SMC stars within a factor of ten of the same far-UV brightness and with O9-B5 spectral types quoted in the literature (M02, Evans et al. 2006, Blair et al. 2009). One of these stars is in the SMC cluster NGC 330 and is listed by Evans et al. as B30. The second star, HV 1620, is a well known O9 eclipsing binary. Two stars are SMC OGLE survey stars that we selected in 2006 for *FUSE* observations. An analysis of these OGLE stars has not been published and we note specifically that the spectral type given in the *FUSE* archives as “B2 V” for OGLE005745.25-723532 was not based on a spectrum and is not to be trusted. The optical spectrum of OGLE005100.18-725303 was discussed and given in M06. Table 4 gives the coordinates,  $m_v$ , and spectral types where possible for these stars. Of these four stars with known far-UV fluxes only the flux of HV 1620 is comparable to the fluxes of our program stars. However, this is a late O star and is clearly not a good match to the far-UV spectra of our program stars. The other three are some 8-10 times brighter, suggesting that they have either earlier types, higher luminosity classes or both. The  $\text{Ly}\beta$  lines and other metallic features in the spectra of the OGLE stars and HV 1620 are weaker than those of our program stars, suggesting that their spectra lie in the O9-B1 range.

In Figure 5 we show a comparison of the spectra over the range 1000-1070 Å for each of the two program stars and NGC 330-B30. Although these spectra are offset for clarity, overplotting them against one another shows that the wings of the dominant  $\text{Ly}\beta$  line are a close match,

**Table 4.** Candidate early-type B stars with FUSE spectra

Object	RA	Dec	$m_v$	Sp. Type
NGC330-B30	00 56-09.4	-72 27 58.9	14.22	B3 III
HV 1620	00 54 38.6	-72 30 04.2	14.08	O9 V + O9 III
OGLE005100.15-725303	00 58 00.1	-72 53 03.9	13.56	B1 II-IIIe
OGLE005745.25-723532	00 57 45.2	-72 35 32.0	13.82	–

suggesting that this star is close to B3 in type. We depict also identifications for 13 available photospheric lines, as taken from the Far-UV Spectral Atlas of B near the Main Sequence (Smith 2010). A comparison of the metallic line ratios of the Si IV and S III relative to the Fe III and Cr III lines, and in turn to the C II 1037 Å line also suggests nearly equal spectral types for B30 and both program objects. In addition, this is also true of the possible luminosity class diagnostic Si III 1113 Å/Si IV 1066 Å (Pellerin et al. 2002, Smith 2010). The value of this ratio is  $\gtrsim 1$  and by itself already suggests a luminosity class in the range III-V. We note again that according to our optical spectra the contribution of the secondary star’s flux must be at least three magnitudes fainter than the primary in the visible wavelength region. This means that the B secondary has  $B$  and  $V$  magnitudes of about 17. This is consistent with the stars’ positions on the upper edge of the main sequence, or approximately luminosity class III and a  $\log g$  of 3.5 to 4. Finally, we point out that the far-UV flux of SMC-SC3 is some 0.57 magnitudes brighter than SMC-SC4, which is probably due to a combination of brighter luminosity and/or slightly earlier type.

With new luminosity class estimates determined, we repeated the spectral synthesis on the C III aggregate at 1176 Å. According to the Pellerin et al. (2002) and Smith (2010) spectral atlases of B stars, this feature undergoes a maximum for B0-B2 V spectra. Spectra of stars just hotter and cooler than this maximum show telltale secondary lines in the wings of this aggregate that allow one to distinguish between an O9 and a middle-B spectral type. We found in our spectra that despite the stars’ low metallicities these features already have strengths close to the maximum exhibited in Galactic spectral standards. In addition, owing to the decrease in Stark broadening, the C III components begin to resolve even for moderate rotations. However, the components are not resolved in our spectra. These considerations suggest that the spectral types are in the range B0-B4. This is in accord with the comparison of the various indicators just discussed. In Figure 6 we exhibit spectra in the region of the C III aggregate compared to B2, B3, and B4 luminosity class V standards. To provide some redundancy we show in Fig. 6b the spectrum of NGC330-B30 as a comparison to SMC-SC4 instead of the Galactic B3 star (Skiff 2009) HD 45047. In both cases the B3 spectrum shows the best match. We also compute and display in this figure the spectrum of the

C III aggregate for a representative photospheric model ( $T_{\text{eff}} = 18000 \text{ K}$ ;  $\log g = 3.5$ ,  $[\text{Fe}] = -0.7$ ). The fit is also good.

If we regard NGC 330-B30 and OGLE005100.18-725303.9 as secondary spectral standards for a low-metallicity early-type B star, the similarity of their profiles with the profiles of our program stars indicate that the profiles of the latter are consistent with isolated stars, although there is a hint of weakening in the C III feature of SMC-SC3. This inference is confirmed by the agreement of the synthesized C III profile with the SMC-SC4 feature, with again a hint of weakening of a several percent in the case of SMC-SC3. The depths of these lines suggest that the contribution of the A primary can be no more than a few percent. We consider it highly unlikely that our targets are interlopers happening to be visible in the *FUSE* aperture. Rather, it appears that the B stars are secondaries with bright giant or supergiant A companions and that they are representatives of binaries caught at similar evolutionary stages. Our discussion of radial velocity variations to follow confirms this inference for SMC-SC4. In this picture the B and A components should have approximately the same stellar mass. In addition, in either of the two wavelength regions where the spectrum of one or the other binary component dominates, we cannot detect the flux from the other.

According to the model atmospheres we used, a B3 V star's flux (assumed to be  $T_{\text{eff}} = 18000 \text{ K}$  and  $\log g = 4$ ) at a wavelength of  $3933 \text{ \AA}$  should be five times the flux of an A5 ( $8500 \text{ K}$ ) of the same radius. Recall that we noted above that we should be able to barely discern a hypothetical 6% contamination to the K line from the B star. This means that the A star has to have a radius of some five times the B star's for the B star not to dilute the K line flux. This is consistent with the stellar radii of middle A supergiants provided that the B star has a radius of  $\sim 7R_{\odot}$ . This gives a radius of  $\sim 30R_{\odot}$  for the A supergiant. This is consistent with values in the literature (e.g., Verdugo et al. 1999) and the mass estimated from evolutionary tracks of  $\approx 9 M_{\odot}$  in M10, and for simplicity we will take  $9 M_{\odot}$  for the secondary mass too. Based on our models, even with its larger radius the A primary should not contribute to the flux at  $1176 \text{ \AA}$ . We conclude from this analysis that each component of these binaries overwhelms the flux of the other in its dominant wavelength regime. The primary conflicting feature with this overall description, as already noted, is the strong  $H_{\alpha}$  emissions in both optical spectra, which is usually an attribute of a Be rather than an Ae star.

### 3.4 Radial velocities

#### 3.4.1 Optical lines

Before conducting a quantitative analysis of the spectral lines in the disk, it was necessary to first identify them and then determine their radial velocities. To obtain radial velocities from the optical spectra, we correlated measured wavelengths of identified lines with their theoretical wavelengths (Kurucz 1993). The results are summarized in Table 5. For SMC-SC4 we give the mean of the “main” (red) component (which is taken as the velocity of the A primary), as well as the velocity of the blue component. To verify the wavelength systems from our Th-He-Ar comparison spectra, we utilized several telluric lines from the oxygen B-band (absorption) and the Galactic ISM component in the Na I D lines. The internal errors, measured by weighting the internal *rms*’s for individual ions, do not exceed  $\pm 4.4 \text{ km s}^{-1}$ , and so we quote  $\pm 5 \text{ km s}^{-1}$ . SMC-SC3 shows a weighted average velocity of 105, 106 and 108 km/s in the 2002, 2007 and 2009 spectra, i.e., it shows virtually no radial velocity (RV) variability. The spectra of SMC-SC4 disclose mean RVs of +100, +108 and +161 km/s at these epochs. Although the RVs are clearly variable, we will exercise considerable caution in interpreting these differences below.

We noticed moderately strong *V* and *R* emission components in the lower members of both the Balmer and Paschen series. The relative strengths of these features decrease to invisibility at  $H_\zeta$ . These lines are flanked by absorption wings. Typically the blue peak is stronger, and they have a deep central absorption. As Table 6 shows, the central absorption cores are found blueward of the centroid of the *V* and *R* emission peaks, typically by  $4\text{--}8 \text{ km s}^{-1}$ . This table displays small differential shifts in these cores as one progresses up the Balmer sequence from  $H_\beta$  and a smaller peak separation at lower order Balmer lines. The Balmer emission decrement is steep, meaning that emissions quickly drop off from  $H_\alpha$  toward the intermediate Balmer lines. All the above are signatures of quasi-Keplerian optically thin  $H_\alpha$ -emitting disks.

In most metallic lines of SMC-SC4, remarkably, we also found sharp blue absorption components (discussed later as “BACs”). These have a blue shift with respect to the primary absorption line components. These shifts average  $-48$ ,  $-50$  and  $-36 \text{ km s}^{-1}$  for the 2002, 2007 and 2009 spectra, respectively. We noticed that in 2009 the BAC is stronger than the main component for the Na D and Fe II group lines.

**Table 5.** Summary of heliocentric radial velocities (in km/s). For SMC-SC4 we give the velocity of the main component and/or the associated BAC. The number of lines included in the averages is also listed. Errors reflect the *rms* of the RVs per line within an ion. For H I we consider central absorptions in the higher level Balmer lines. The mean RVs exclude He I lines.

Ion	SMC-SC3	SMC-SC3	SMC-SC3	SMC-SC4	SMC-SC4	SMC-SC4
	2002	2007	2009	2002	2007	2009
CaI	-	108±12 (2)	-	-	-	-
CaII	-	106±5 (5)	111 (1)	-	53±7 (2); 109±1 (2)	-
CrII	106±8 (5)	107±11 (10)	105±6 (8)	48±10 (3)	55±11 (6); 101±10 (3)	125±9 (5); 164±9 (8)
FeI	105±6 (11)	110±12 (27)	116±10 (4)	52±5 (10); 97±3 (3)	50±3 (2)	168±5 (11)
FeII	104±10 (22)	106±3 (41)	109±3 (37)	51±9 (16); 103±4 (11)	54±5 (21); 105±6 (30)	119±3 (14); 167±7 (23)
H I	105±3 (18)	106±3 (28)	-	106±3 (16)	106±6 (28)	-
HeI	37±0 (2)	-	27±3 (2)	-	-	-
MgI	105±2 (3)	103±6 (3)	110±1 (2)	54±4 (3); 97±4 (3)	58±1 (2); 104±3 (2)	130±1 (2); 162±2 (2)
MgII	-	115±24 (3)	-	-	48±16 (4); 94±4 (3)	156± 2 (3); 175 (1)
ScII	-	109±5 (2)	113±1 (2)	52 (1)	69±7 (2)	-
SiII	105±2 (4)	106±27 (7)	116±9 (4)	55±4 (2)	67±10 (5); 119±13 (2)	169±7 (5)
SrII	-	106±13 (2)	-	-	60±2 (2)	172±5 (2)
TiI	-	98±26 (7)	107±5 (3)	-	48±12 (7)	164±10 (5)
TiII	106±2 (7)	105±7 (35)	108±4 (22)	50±5 (10); 96±5 (5)	52±7 (6); 111±16 (9)	129±5 (14); 170±15 (12)
mean	105 ± 1	107±4	111±4	52±2; 100±4	56±7; 106±7	126 ± 5; 166 ± 5
w. mean	105	106	108	53; 100	58; 108	129; 161

**Table 6.** Heliocentric radial velocities (in km/s) for H I emission line components and shift of the central absorption relative to the centroid of the red and violet emission peaks for years 2002/2007/2009. NP means not present. Note the larger peak separation ( $\Delta\lambda$ ) in higher order lines.

Emission line	star	blue-peak	central-abs	red-peak	shift	$\Delta\lambda$ (km/s)
H $\delta$	SMC-SC3	-/20/NP	-/107/106	-/172/NP	-/-2/-	-/152/-
H $\gamma$	SMC-SC3	-/31/21	-/93/92	-/168/190	-/-6/-14	-/137/169
H $\beta$	SMC-SC3	24/32/27	95/92/94	159/166/160	-4/-7/1	135/134/133
H $\alpha$	SMC-SC3	55/46/41	93/91/91	153/152/142	-11/-8/-1	98/106/101
H $\delta$	SMC-SC4	-/NP/NP	-/104/140	-/NP/NP	-/-/-	-/-/-
H $\gamma$	SMC-SC4	-/NP/48	-/106/110	-/NP/NP	-/-/-	-/-/-
H $\beta$	SMC-SC4	46/NP/-	105/112/101	183/181/185	-16/-/-	137/-/-
H $\alpha$	SMC-SC4	55/64/51	114/111/106	171/165/170	-1/-4/-4	116/101/119

### 3.4.2 Far-UV lines

We used the Far-UV Spectral Atlas of B Stars Near the Main Sequence (Smith 2010) to identify a number of lines in our *FUSE* spectra to measure radial velocities of the B stars at the time of our observations. The results for SMC-SC3 and SMC-SC4 are  $+138 \pm 12 \text{ km s}^{-1}$  and  $+136 \pm 15 \text{ km s}^{-1}$ , respectively. *FUSE* spectra are prone to several systematic sources of errors in their wavelength calibrations (Dixon et al. 2007), and thus the zeropoint differences may easily be as large as  $\pm 20 \text{ km s}^{-1}$ . Nonetheless, we noticed that the measured wavelengths of the same lines for the same spectra closely coincided in nearly all cases. On the basis of the spatial positions of the two dimensional spectra, we believe the apertures were placed consistently over the stellar images and that the radial velocity difference between the B star spectra is no more than  $10 \text{ km s}^{-1}$ .

### 3.5 Spectral synthesis methodology

Much of the analysis in this paper relies on spectral line synthesis, so we first describe the methods used for this analysis. We have adopted the results of the fitting of the wings of the Ca II K-line and assumed stellar parameters for SMC-SC3 and SMC-SC4, namely  $\log g = 2.5$  and 3, which are appropriate for luminosity class I and II mid-A stars, respectively, and a metallicity of  $0.2 \times$  solar (e.g., Dolphin et al. 2001, Mighell et al. 1998, Dufton et al. 2005). The spectra were analyzed using the SYNSPEC and CIRCUS (disk) spectral synthesis programs (Hubeny, Lanz, & Jeffery 1994, Hubeny & Heap 1996).

Using CIRCUS, we were able to estimate rotational broadenings,  $V \sin i$ , from the absorption lines in both the *FUSE* and optical spectra of our two program stars. For SMC-SC3 the A primary and B secondary have broadenings of  $20 \pm 5 \text{ km s}^{-1}$  and  $50 \pm 10 \text{ km s}^{-1}$ . For SMC-SC4 the corresponding rotational broadenings for the A and B binary components are  $28 \pm 5 \text{ km s}^{-1}$  and  $75 \pm 10 \text{ km s}^{-1}$ .

For CIRCUS analysis one must assume an input temperature for a putative intervening disk structure,  $T_{\text{disk}}$ , and several other parameters. The CIRCUS program permits as many as three separate absorbing or emitting regions to be specified, each with its own areal coverage, local temperature, and radial velocity. We utilized this feature in some cases to specify two distinct temperature regions, since the line identifications indicated that the lines we modeled arise in regions having a temperature range of 5-8 kK. At these temperatures the fraction of the ions considered plateaus, and thus the errors in this parameter are not large. The strengths of disk components of the Na D and K I profiles can be most easily modeled by temperatures of 5 kK or less, consistent with the picture from the  $H_\alpha$  emission profiles of the disks extending out to at least several stellar radii. Nonetheless, our models show that the column densities required to fit these components decrease monotonically with temperature. Thus these values are not well constrained. The strengths and widths of the Fe II and Si II lines suggest a microturbulence  $\xi$  of about  $10 \text{ km s}^{-1}$ , and we assumed the disk to be approximately Keplerian. For lines having both photospheric and circumstellar components, these components exhibit no net shift. Therefore, the latter structure appears to be in a Keplerian orbit. We have also assumed that the foreground disk segment fully covers the star. However, if our lines of sight toward different portions of the star sample different disk conditions along the way, our column densities will be underestimated.

These assumptions required the matching of the computed equivalent widths to the observations using a one or two parameter fit in disk and column densities. The columns needed to fit the

observed line strengths and the strength ratios of lines arising from the same ion indicate that the strong disk lines we measured are optically thick. In some cases the lines are observed to have peak equivalent widths (EWs) as large as we can compute them even from assumed optimal conditions. We note also that for the optical strong Fe II lines, we fit *emission* profiles in our models with temperatures for a medium with a larger projected area than the star's - that is, as if they are formed in lines of sight that do not intersect the star disk. We will express the column densities in examples below by using the unit “stellar area.”

Our modeling represents an oversimplification of the true and unknown disk conditions because the disk geometry and velocity fields are poorly known. In addition, the computation of line strengths requires a common estimated excitation and ionization temperature. Nonetheless, for exploratory purposes we believe that our models provide insight into the thermal and velocity differentiation within the disks. Generally, departures from LTE in the line transitions will result in an underpopulation of the higher levels relative to lower and resonance levels, and therefore an increase in the absorbing column density for lines arising from excited levels. We have computed our absorption column densities in this scattering approximation in our CIRCUS simulations.

### 3.6 The disk features in SMC-SC3

In view of the implied complex nature of the structures surrounding both program stars, we will discuss quantitative fits to several line profiles mainly to get an idea of the column densities, radial velocities, and turbulences in the disk gas. Except for a model fitting to the excited He I line and resonance lines (which form in cold media which we cannot specify accurately), we will limit our quantitative analysis to the optical metal lines arising from atomic levels of a few eV. Because of the uncertainties involved, we discourage the reader from not interpreting our numerical results too literally.

Nearly all the features in the optical spectra of SMC-SC3 are characteristic of absorptions in an extensive and flattened, differentiated disk or envelope. The high-level Balmer and Paschen lines can be resolved out to H30 (Fig. 1a) and P24, but any disk contribution to them cannot be well determined because these features are common in A supergiants spectra. Our SYNSPEC simulations of these high atomic levels lead to estimates for the characteristic density in the line formation in the atmosphere of  $1\text{-}3 \times 10^{11} \text{ cm}^{-3}$ .

In our initial modeling we discovered that the disk temperature and therefore the column density through the disk along the line of sight cannot be constrained to a single temperature, partic-

ularly for metallic absorption lines in the blue/near-UV region. For example, given assumed disk gas temperatures values of 6 kK and 5 kK, we are able to generate good CIRCUS fits to weak lines in the 3800-3850 Å region in our spectra with column densities of about  $3 \times 10^{22} \text{ cm}^{-2}$  or  $7 \times 10^{21} \text{ cm}^{-2}$ , respectively. These values carry uncertainties of at least a factor of three and assume full disk coverage of the star. We were able to get a better handle on these parameters by finding a region of the spectrum at 5250-5280 Å that contains both Fe I and Fe II intermediate strength lines. Our modeling for the region of 5250-5280 Å is depicted in Figure 7. The ionization temperature in the disk is already well constrained by the Fe I/Fe II ratio to be  $\approx 7$  kK. However, we found that to reproduce also the observed strengths of the features with a metallicity and column densities obtained for fits of our other line requires that lines of each ion be formed in media that favor each of their ionization states, rather than an intermediate value near 7 kK. We were able to obtain reasonable fits for both disk spectra with a two-component model having  $T_{\text{disk}} = 6$  kK and 8 kK. (In reality this means that the disk is described by a continuous distribution warm to cooler temperatures.) The column densities given in Fig. 7 are generally a few times  $10^{22} \text{ cm}^{-2}$ , consistent with our less refined analyses of the lines in the far blue.

A salient attribute of the strongest Fe II lines of SMC-SC3, (which arise from a common multiplet having 2.9 eV) is that they exhibit broad absorption components and even broader emissions. Certainly, the emission components and even much of the absorption does not appear to be photospheric. For example, among the strongest three lines, 5169 Å, 5018 Å, and 4923 Å the stronger the line, the more pronounced the absorption and overlying emission wings, a point which we now elaborate.

Among the strong disk Fe II lines in this spectrum, we chose to fit the 5018 Å line, which is depicted in Figure 8. Our fit for this feature was achieved by confirming the column density of a disk from the emission component of a few Fe II lines. These lines are 4923 Å, 5018 Å, 5169 Å, 5316 Å. We estimated from their relative emission strengths that they are mildly optically thick,  $\tau_L \sim 3$ . For the optical spectrum of SMC-SC3 this corresponds to a column density of  $3 \times 10^{22} \text{ cm}^{-2}$  and a temperature of 8 kK. This is the same temperature and nearly the same column density as we found for the lines in Fig. 7. This agreement allowed us to fit the absorption features of these Fe II lines straightforwardly. The full profile was fit in CIRCUS with a two temperature-component simulation. We fit the emission using the same column density and temperature as just found for the absorption component. Next we needed to broaden the simulated emission feature by a gaussian macroturbulence of  $70 \text{ km s}^{-1}$ . The amplitude of the emission required adding a free parameter, the emitting gas area, which we found to be 11 stellar areas in this case. We note here

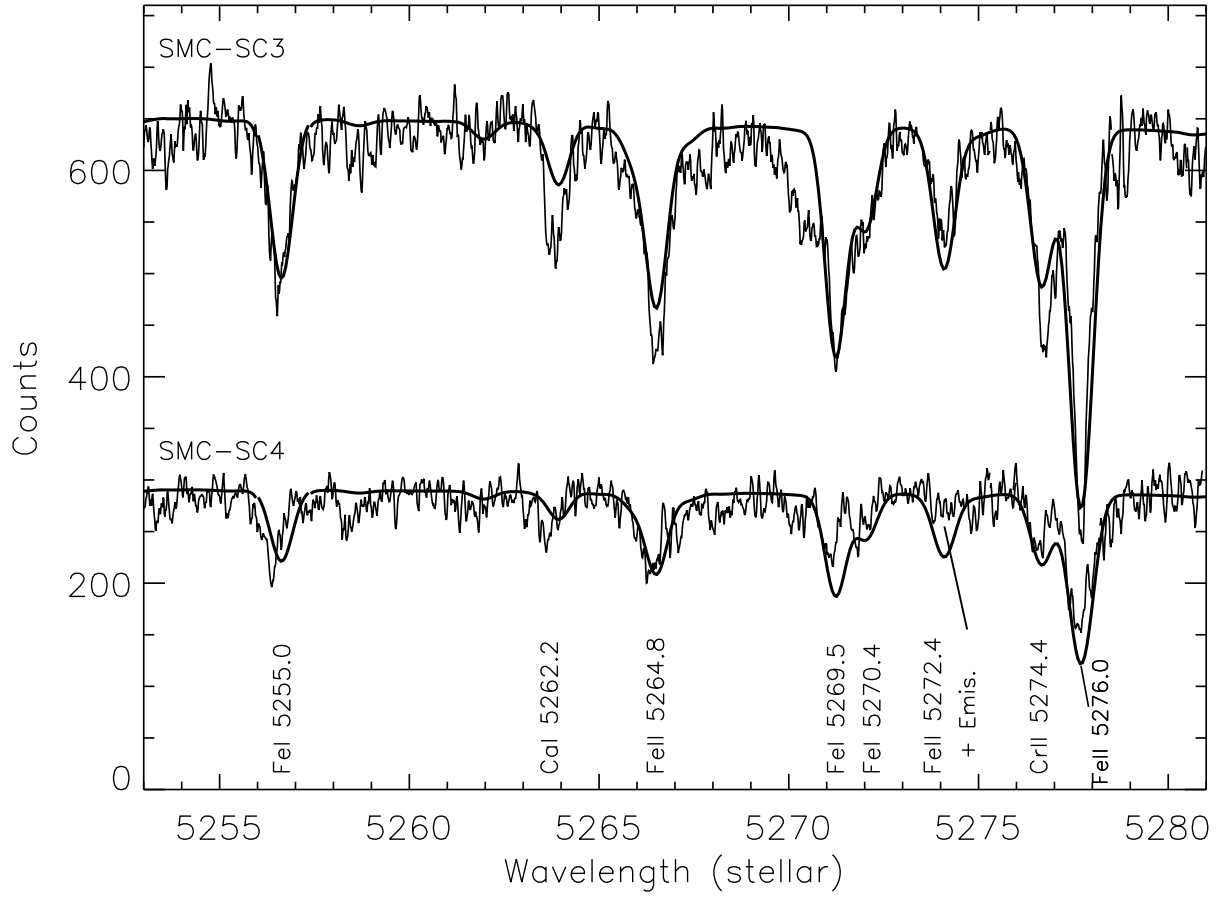


**Figure 7.** The fit of yellow Fe-like lines for SMC-SC3 (upper) and SMC-SC4 (lower) of our UVES spectra to a two-temperature (8 kK, 6 kK) model. For the warmer component the column densities were  $5 \times 10^{22} \text{ cm}^{-2}$  and  $2 \times 10^{22} \text{ cm}^{-2}$  for SMC-SC3 and SMC-SC4, respectively. The columns for the cool component were  $3 \times 10^{22} \text{ cm}^{-2}$  and  $1 \times 10^{22} \text{ cm}^{-2}$ . The weak feature appearing at redshifted wavelength 5258 Å, not present in our simulation, is likely to be an Fe I line the published oscillator strength of which is inadequate. The Fe I 5255 Å line arises from a 10 eV level. In the SMC-SC4 this feature exhibits weak redshifted emission.

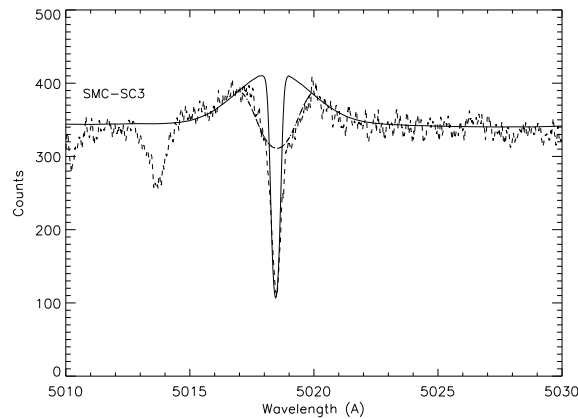


**Figure 8.** A fit of the Fe II 5018 Å line (UVES spectrum) for SMC-SC3. This profile was fit by two independent models, one with a temperature of 8 kK (see text for other details). The second component was fit to the emitting wings with the same gas temperature and by assuming an area of 11 stellar areas and a gaussian turbulence function of  $70 \text{ km s}^{-1}$ . Wavelengths are in the observed system for the 2002 epoch.

that we actually have no independent handle on the volumetric density of the matter in which the Fe II lines are formed. Using the column lengths of  $\sim 3R_*$ , characteristic of the derived emitting areas ( $\sim 11$  stellar areas), we can estimate characteristic densities of  $3\text{--}10 \times 10^9 \text{ cm}^{-3}$ . Values of this order of magnitude should not result in visible forbidden features, and indeed they are not seen.

The Si II and O I triplet in the SMC-SC3 spectrum are formed in plasma with temperatures in the range 6–9 kK as well. Although their cores are sharp, and consistent with being formed in a medium distant from the star, their strong wings suggest a second component formed closer to the star. The Na I D and K I multiplets in this spectrum have the same combination of sharp core and extended wings. This is also true for several of the Fe II lines and the Si I 6347 Å, 6371 Å doublet, which have high optical depths and therefore characteristic mean formation sites in the outer disk where the temperature and column length are low. For the Na I and K I lines we could fit the line cores with a column above the photosphere of  $5 \times 10^{21} \text{ cm}^{-2}$  for  $T_{\text{disk}} = 4 \text{ kK}$  and  $1.5 \times 10^{22} \text{ cm}^{-2}$  for 5 kK.

We address next the remarkable emissions in the He I 5876 Å, 6678 Å, and 7265 Å lines, all of which arise from 21 eV levels. We show the stronger of these lines, 5876 Å and 7265 Å, in Figure 9, corrected for their mean redshift of  $32 \text{ km s}^{-1}$ . These lines are the only ones in the spectra of both stars that differ markedly from the other line system(s). The observed 5876 Å/6678 Å line emission ratio is about 3 to 1, which suggests that these lines are formed in an optically thin medium. Such emissions are typically produced in a relatively dense plasma by heated gas, such as in shocks, or in much more energetic astrophysical venues (like winds of Be X-ray binaries) by recombination. Our simulations show varying efficiencies of formation in media of 15 to 23 kK, with corresponding emission regions encompassing of 8–12 to 3–4.5 stellar areas and column densities of no more than  $1\text{--}5 \times 10^{22} \text{ cm}^{-2}$  for the two respective gas temperatures. If this heated gas undergoes continuous cooling down to 8 kK, it is likely, given the small volume of formation implied by the He I emission widths, that the resulting emission generated in the Fe II lines would be hidden by the much broader Fe II emission component formed over the larger disk volume.

### 3.7 The metallic line features in SMC-SC4

Much of what we found for SMC-SC3 is true also for SMC-SC4, and we have already pointed out that the inferred temperature distribution for the disk around SMC-SC4 is indistinguishable from the SMC-SC3 disk. For the most part the column densities in our fits to the main (unshifted) metallic absorption line features run a factor of two to three times lower. For example, for a 6 kK

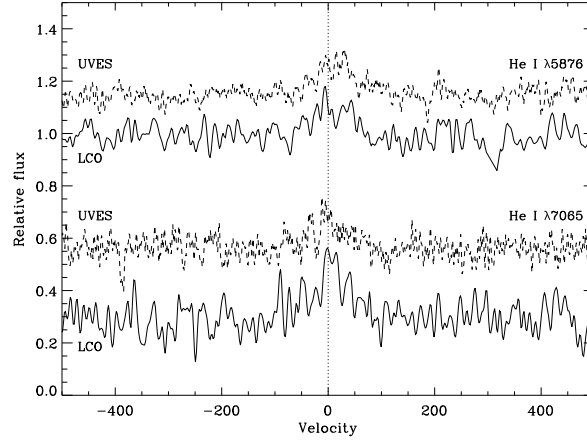


**Figure 9.** The regions of the He I 5876 Å and 7065 Å weak emission lines in the spectrum of SMC-SC3 in both UVES (2002) and LCO (2009) spectra. Here the velocity zeropoint is taken as the mean,  $-32 \text{ km s}^{-1}$ , noted in Table 5 and is  $-74 \text{ km s}^{-1}$  from the average velocity of the features in the optical spectrum. Note the near absence of velocity shifts between the two. The fluxes are 4-point smoothing of the raw data.

model the 3800-3850 Å lines could be fit with column densities of about  $7 \times 10^{21} \text{ cm}^{-2}$  and the Fe II lines in the 5250-5280 Å region by some  $2 \times 10^{22} \text{ cm}^{-2}$ .

### 3.7.1 Blue Absorption Components (BAC)

Most of the strong lines in this spectrum have profiles different from those of SMC-SC3. The most noticeable difference is the presence of one and sometimes two discrete BACs in the SMC-SC4 spectrum. These “BACs” are so named because their morphology is reminiscent of the “DACs” in resonance lines of radiation-driven winds of hot stars. A primary BAC generally occurs at about  $-50 \text{ km s}^{-1}$  to the blue of a redder or “main” component, which we so name because the latter’s velocity are coincident with the RVs of the high level Balmer lines. The double entries in SMC-SC4 columns of Table 5 indicate the commonness of single BACs throughout the optical spectrum.

The yellow optical region is rich in intermediate strength Fe II lines with  $\chi \approx 3 \text{ eV}$ , and these lines show prominent BAC strengths. For example, the fitting of BACs in the 5018 Å line in the UVES spectrum required column densities of  $3\text{-}10 \times 10^{22} \text{ cm}^{-2}$ , or several times that of the main (static) components. This is largely because these components are mildly optically thick. The pattern of two BACs is common among the strongest of these 3 eV Fe II lines. Figs. 11a and 11b exhibit double component pattern in the 5018 Å and 4923 Å lines, respectively. In both figures a “secondary” BAC shifted by about  $-100 \text{ km s}^{-1}$  relative to the main (red) component is conspicuous. The BAC strengths for the Fe II lines can change over time, and Fig. 11a shows changes for the 4923 Å line. As expected, the strengths of BACs among various lines arising from the same ion and comparable excitation levels increase with line strength.

BACs are relatively weak in lines arising from near-ground state atomic levels in low ioniza-

tion species such as Mg I, Fe I, and Ti II. They are particularly noticeable in lines arising from moderately excited states of abundant metallic ions like Fe II, Mg I, Si II and even the O I 7771-5 Å triplet (9 eV) - see Figure 10. The excited lines in the NI 8703-48 multiplet ( $\chi=10$  eV) exhibit a similar behavior as the O I triplet. Many of the strongest lines, including the high order Balmer lines, and the Na I D and KI 7699 Å doublets at first seem to show a shading toward one wing or the other, depending on the epoch. However, as the 2007 MIKE spectrum makes clear in Fig. 2, this tapering is due to the blending of two BACs. In this spectrum the “tapering” is fully resolved into two sharp components.

### 3.7.2 Ephemeral non-BAC features

In addition to BACs, absorptions and emission components appear often in the extreme wings of the Fe II lines. However, their behavior is in some respects stranger than the BACs. Both panels of Fig. 11 show that the flux in one of the wings can change from absorption to weak emission among members of the same multiplet in the same spectrum. The difference in the fluxes in the red wings of the 4923 Å and 5018 Å lines is particularly surprising because their difference in  $\log gf$  is only about 0.1 dex. These differences can be seen even more dramatically in Figure 12a, again in the same spectrum. Note in the blue wing the strongest line in a multiplet, 5169 Å, shows absorption. As one proceeds to the weaker members in the series, e.g., 5316 Å, the wing exhibits the *strongest* emission.

The increased activity with time for the “weak” 5316 Å line is exhibited in Figure 12b. This figure also shows weak absorption in the red wing, i.e., the opposite wing in which emission is seen. Other lines show this same behavior (e.g., Fig. 11b).

As one proceeds to higher excitation lines the secondary BACs disappear, and often so do the main components. Figure 13 shows vestigial red wing emissions of the excited Si II 6347 Å, 6371 Å doublet similar to those just exhibited in the Fe II 5316 Å profile in Fig. 12b.

In Figure 12a we point out the curious difference between the BAC and emission strengths of the same 2009 spectrum: whereas the strengths of BACs of lines in the same multiplet or super-multiplet increase as expected with oscillator strength, the strengths of the emissions go in reverse order, that is, the strongest line ( $\lambda 5169$ ) shows blue wing *absorption* and the weakest line shows the strongest emission. This is depicted in Fig. 12a, and the reversal can be seen in spectra from other epochs as well. *This behavior sets the far wing features apart phenomenologically from the BACs.*

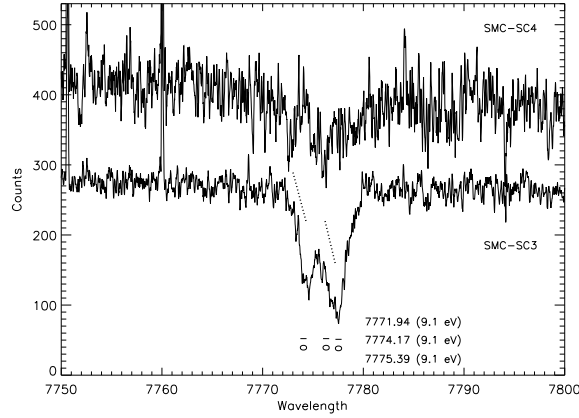


**Figure 10.** Comparison of the OI triplet in the two program stars (UVES spectra). These lines, located at 7771.94 Å, 7774.17 Å, and 7775.39 Å, arise from a level at 9.1 eV. Note the broadening and the sharp, blueshifted BAC components in the SMC-SC4 spectrum.

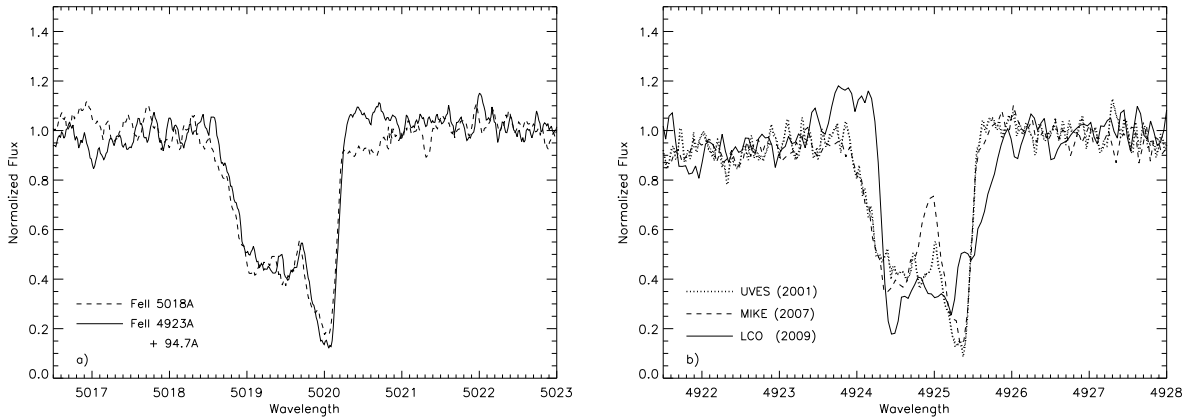


**Figure 11.** Panel (a): Overplotting of the Fe II 4923 Å and 5018 Å lines from the UVES spectra of SMC-SC4, exhibiting *two* Discrete Blue Absorption Components (‘BACs’). The 4923 Å line was redshifted by 94.7 Å. The red wing absorption (5018 Å line) and emission (4923 Å line) discussed in the text are present in this figure. MIKE (2007), and LCO (2009) spectra of the Fe II 4923 Å profile. The 2007 and 2009 spectra have been shifted to force the major absorptions to coincide. Red wing absorption and blue wing emission are present in the 2009 spectrum.

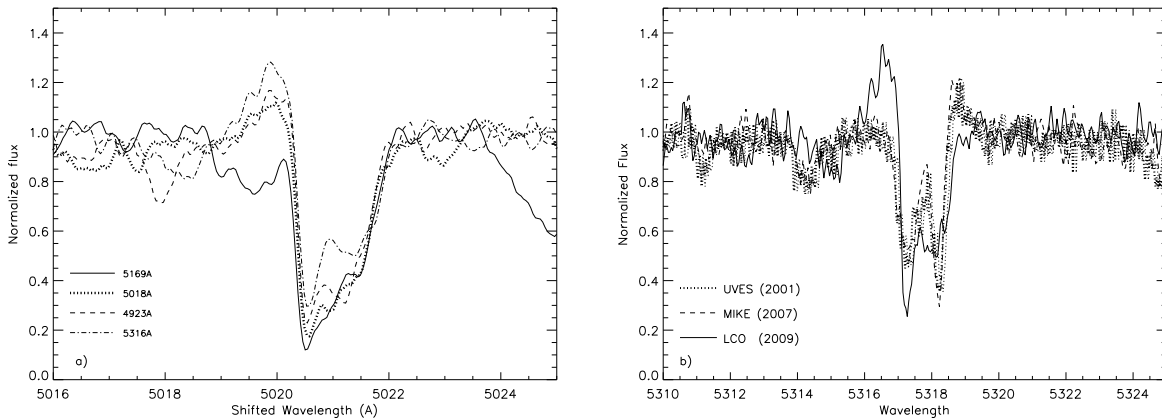


**Figure 12.** (a) Overplotting of Fe II 5169 Å, 5018 Å, 4923 Å, and 5316 Å (in order of decreasing strength) in the LCO (2009) spectrum. Each of the other profiles have been coshifted to the wavelength centroid of 5018 Å. Note the increasing flux in the blue wing at 5019-5020 Å with decreasing line strength. (b) The Fe II 5316 Å line of SMC-SC4, exhibiting *two* BACs; the MIKE (2007) and LCO (2009) spectra have been shifted in wavelength to force the major absorptions to coincide. The emission activity at 5316.5 Å and 5318.5 Å is discussed in the text.

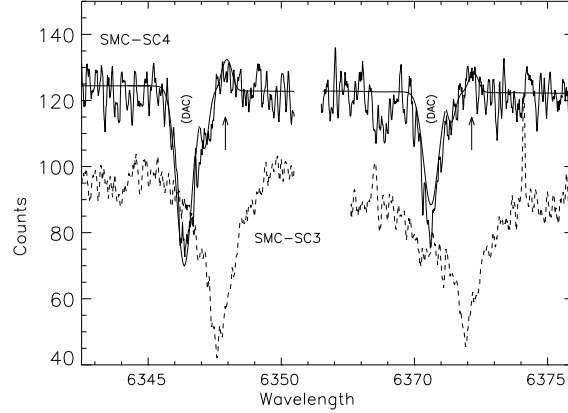


**Figure 13.** A fit to the Si II 6347 Å and 6371 Å doublet (solid line) of the UVES (2002) spectrum, emphasizing the BACs and the filled in main components for the SMC-SC4, such as also found in other strong Fe II lines and the excited Fe II 5255 Å line (e.g., Figs. 7, 11 & 12a). The observed spectrum is depicted for SMC-SC3 in order to guide the eye to the filled in red wing emission in the SMC-SC4 spectrum. The solid line fit was attained with a model having a disk temperature of 8 kK, a column of  $3 \times 10^{22} \text{ cm}^{-2}$ , and a projected surface of 1 stellar area. The 6371 Å profiles have been shifted by  $-14.9 \text{ Å}$  with respect to the 6347 Å for convenience.

We end this section by reporting that we encountered difficulties in attempting to fit the Fe II line emissions strengths of Fig. 12 with our CIRCUS models, even though it was easy to fit a similar emission in the Si II profiles shown in Fig. 13. The source of the problem is the combined constraints affecting the formation of the Fe II lines. As one increases the gas temperature in the models the Fe II emissions increase up to a point. However, above 9 kK the flux emitted by a given gas volume decreases rapidly as the ionization of iron shifts to  $\text{Fe}^{++}$ . Above this temperature, regardless of the column density (the lines are optically thick already), the emission requires increases in the emitting volume and therefore the area. In practice, an emitting area of at least 10 stellar areas is required – substantially higher values are needed for gas temperatures greater than 10 kK or less than 8 kK. These simulations bring out a contradiction according to our assumptions: *whereas the blue wing absorption in the strong  $\lambda 5169$  line can be formed in columns subtending no more than one stellar area, the emissions of Fe II lines in the same multiplet must be produced in substantially larger areas and volumes and possibly different temperatures.* Clearly the formation of various components of the Fe II lines in this spectrum occurs in separate regions having diverse properties. We will return to this point in the next section.

## 4 DISCUSSION

### 4.1 General

The primary attributes that initially drew our attention to the program stars were their multiple periods in the OGLE *I*-band light curves. However, it was the complex nature of their optical

spectra even at moderate resolution that led to this detailed spectroscopic analysis. We have already noted the strong double-peaked emission in  $H_\alpha$  and other low members of the Balmer series, which is uncharacteristic of an A star, even one of high luminosity. The acquisition of far-UV spectra has clarified that these objects are A + B luminous binaries, and three optical spectra have confirmed radial velocity variations for SMC-SC4. The current investigation discloses no new clues to the origin of the 15 day period of SMC-SC3 or of the “chaotic” photometric activity for SMC-SC4 discussed in M10. However, we can remark further on spectroscopic activity pertinent to the 184 day “eclipse” period.

In §3.3.1 we expressed doubts as to how far the RV variations from the optical lines of SMC-SC4 can be interpreted. For example, given the extreme changes in line profiles in the 2009 spectrum, it is not clear that we can trust the cross-correlation among spectra of different epochs to faithfully represent the motion of the A star around its orbit. We also note that in the only blue Balmer line covered in all three observations,  $H_\delta$ , the wings suggest that the RV variations are larger than  $100 \text{ km s}^{-1}$ . For this reason we do not trust these few measurements to estimate binary orbit attributes such as eccentricity and inclination reliably. Nonetheless, reasonable to infer that the RV variations are due to the same 184 day eclipse period discussed by M10, even though the eclipses are almost certainly not due to the secondary star. We will comment on further on this geometry in §4.4.

If one adopts Kepler’s Third Law for the SMC-SC4 orbit  $18 M_\odot$  and a 184 day binary period, one finds a semimajor axis for the binary system of 1.66 AU. Considering next the disk, if one assume Keplerian orbits and adopts a measured separation between the V and R emission components in the  $H_\alpha$  profile of  $110 \text{ km s}^{-1}$ , the characteristic orbital radius for the disk becomes  $4.9 \sin^2 i$  AU. Furthermore, the well resolved nature of the two emission peaks implies once again that the  $\sin^2 i$  factor is not far from unity. Then assuming further only that the disk and orbital planes are at least roughly coincident, the ratio of the size of the disk to distance between the stars is about a factor of 2-3 ( $4.9 \sin^2 i / 1.66$ ). The conclusion is that in fact the emitting gas arises in a *circumbinary* (CB) disk around the SMC-SC4 system. Confirmation of this picture comes from the fact that the V/R emission ratio of the  $H_\alpha$  profile of SMC-SC4 changes from the 2002 to the 2007 epoch even at near-like binary phases. We would expect the details of the emission profile to be different if the emission came from the environment of one of the binary components. We use the descriptor “circumbinary” hereafter to describe the structure causing the disk emission and most of the exophotospheric absorptions in its spectrum. We have not made the case for RV variability

for SMC-SC3, but given the discovery of its B secondary this seems to be a matter of discovery given our poor phase sampling.

As for SMC-SC3, if one again takes the sum of masses as  $18M_{\odot}$  and a period of 238 days, one derives a semimajor axis of 5.4 AU of the system. This is larger than the scale of the SMC-SC4 system, but then the  $H\alpha$  emission is some four times stronger for SMC-SC3 (Table 3), which implies a more extensive disk outside this radius.

Altogether, the high resolution spectra have revealed a number of novel properties that are different for each star and yet reminiscent of one another. The two stars, and the overarching question is how the evolutionary state of the binaries and the remarkably slow rotations of the component stars might be responsible. These novel properties include emission, the unusual excitations implied by the emissions in He I (SMC-SC3 only), Si II, and Fe II lines, and for SMC-SC4 the presence of multiple components, including “BACs” in the strong resonance and intermediate strength lines, and emission components in permitted Fe II and Si II lines,

Before evaluating the spectra of our program stars further, we should state our assumptions about the dynamics of the binary-wind system that will facilitate consideration of the simplest possible picture that at the same time is consistent with the complex features we see. Because of their presume relatively high space density in the region of the SMC first investigated, we assume that both program stars are immediately post-main sequence. We have also assumed that  $M_2 \approx M_1$ , and this is based on the absence of any evidence of extensive mass transfer, anomalous abundances, or rotational spin up. The stellar radii we determined particularly from the surface gravities inferred from the Ca II and C III lines suggests that the stars’ radii are much smaller than their Roche lobes. This leads to the simplifying picture that, except for wind-wind or wind-CB disk interactions, the wind kinematics and geometries are not differ radically from those of single stars. Of course, the fate of wind efflux stopped by collisions with the other wind or a disk, as suggested by shock features, suggests a more complex scenario. We assume that the residual momentum of the B star wind forces some of this stalled matter to the A primary, perhaps in a relatively narrow neck defined by the inner Lagrangian point. If any matter also returns to the B star it would not be observed in our optical spectra.

## 4.2 The emission features in the SMC-SC3 spectrum

The  $H_{\alpha}$  emissions in both program stars are strong but not at the high end of the range among classical and pre-main sequence Be stars. The presence of  $H_{\alpha}$  emission has long been used to

confine the cool limit “Be phenomenon” in the HR Diagram. Jaschek et al. (1988) have surveyed a large number of Galactic Ae stars, and even the class most resembling our program stars in having a rich optical shell spectrum, their “Group II,” is confined to types A0-A1. The emission profiles of those early A supergiants are weak, transient, and have a P Cygni, or inverse P Cygni, shape (e.g., Verdugo 2005), characteristic of activity close to the stars’ surfaces. For our program objects the continuum fluxes of the B secondaries are several times smaller in the red than the primaries’ fluxes. It strains credibility to imagine that the A stars or for that matter the B stars’ photospheric UV fluxes can excite such strong emission. Emission in the  $H_\alpha$  line is invariably generated by recombination in dense circum-stellar/binary environments of hot stars. Yet the extended wings of these features hint at the importance of electron scattering, and this implies that the disk extends to low densities and large radii.

The presence of  $V$ ,  $R$  emissions in strong Fe II lines of SMC-SC3 is a characteristic in a number of well-known classical Be stars. These spectroscopic signatures are formed by scattering in dense, high optical-depth disks as well. An important characteristic of these emission profiles is that they remain almost symmetric in our observations, suggesting a stationary disk. However, a small persistent excess in the  $R$  emission may hint at a few  $\text{km s}^{-1}$  expansion of this structure. Separate from these considerations, the superposition of broad absorption profiles of strong Fe II (e.g., Fig. 8) and other excited lines like the Si II doublet suggests the presence of a separate absorbing source close to the A star component of SMC-SC3.

A clue to understanding the energetics of the disk of SMC-SC3 is the presence of He I lines from the primary’s photospheric and circumbinary lines. As with the hydrogen emissions, these lines cannot be excited by the photospheric radiation field. A ready alternative is the shocks provided between wind-wind collisions between the stars. In the absence of profiles of the UV resonance lines, this is still a speculative idea. Nonetheless, the fact that the velocities of the He I lines are so different from all the absorption line velocities indicates that they are formed in a different physical region that need not even be confined to the disk plane. From our fittings of the strengths of He I (§3.5), we found that for plasma heated to 18 kK, a column length of  $3 \times 10^{22} \text{ cm}^{-1}$  is typical. Adopting a value of  $N_e \sim 10^{11} \text{ cm}^{-3}$ , typical of CS disks of Be and Ae stars, the column length implies a radial extent of  $3 \times 10^5 \text{ km}$  ( $\sim 2\%$  of the A star’s radius) for the formation region; if the temperature this extent could be much less. This is consistent with shock formation and inconsistent with mechanisms that excite helium atoms over a large volume, e.g., irradiation by X-rays.

### 4.3 BACs and related features in SMC-SC4’s optical spectrum

The kinematics of the disk surrounding the SMC-SC4 system are quite different from the SMC-SC3. For example, the metallic lines do not show a symmetric two ( $V$ ,  $R$ ) component emission that suggests the presence of a stationary disk nor that the optical depths of the circumstellar or circumbinary absorptions have as high optical depths. In contrast, there are the blue and occasionally red absorption components, as well as emissions in the wings of the main line whose positions seem to be determined by the orbital phase.

Although ubiquitous, novel, and likely present at all orbital phases, the BAC features are not unique to the SMC-SC4 system. In a little noted discovery, Heydari-Malayeri (1990) reported that many of the metallic absorption lines in the optical spectrum of the SMC supergiant N82 consist of double components, the dominant member of which is blueshifted by about  $-46 \text{ km s}^{-1}$ . This is almost the same value found for SMC-SC4. The Balmer lines also show double-peaked emissions intermediate in strength between those we find SMC-SC3 and SMC-SC4. In addition, Heydari-Malayeri found that lines of different ions have various red to blue emission component ratios. This caused the RVs of members of ions exhibiting these components to have a large RV scatter. This author classified N82 as a “sgB[e]” star largely on the basis of the presence of infrared emission and the appearance of [Fe] emission lines. However, an important supporting justification for the author’s classifying N82 as Be rather than Ae was the star’s strong Balmer line emissions. Because we now know that this is not necessarily a *sine qua non* criterion for Be classification, the argument that this object is a B star is weakened. The presence of [Fe] emission in the spectrum of N82 but not in our program star spectra suggests that N82’s attributes are phenomenologically distinct. However, its spectrum is similar in including BAC components in metallic lines and substantial emission in the lower Balmer lines.

Overall, the striking attributes of the BAC-like components in the SMC-SC4 spectrum are: *a*) their ubiquity among many types of lines, *b*) their consistent blueshifts of  $-50$  to  $-32 \text{ km s}^{-1}$  in at least three orbital phases, and *c*) their concentration mainly among lines arising from atomic levels of a few eV. Points *a* and *b* argue that the BACs appear the same around the orbital cycle and are perhaps caused by impacts of an axisymmetric outflow.

We also found, depending on the epoch, that absorptions in either the far blue or red wings of some Fe II lines show an extraordinary sensitivity to excitation and line strength. The flux in emission features exhibits a reversed dependence on the line’s oscillator strength, with the weaker lines showing the greater emission. The sensitivity of emissions to line strength fits in with the

shock hypothesis because it implies a rapid increase in local temperature, perhaps over only  $10^4$  km in the case of the 3 eV Fe II lines, in the formation length where the emissions of (weaker) lines are formed. The sensitivity to line strength and excitational information also hints that the energy input into the putative shocks has a small “bandwidth,” that is, if the outflows were less or more energetic than some other range of excited states would be collisionally populated. This is consistent with the wind energetics because winds have a characteristic velocity when they impact stationary matter at a fixed distance. According to these ideas, one expects the excitations of atoms exhibiting emission to depend on the wind velocities, and thus to some degree also the orbital separation between the stars. Perhaps these conditions are “just right” for SMC-SC3 to excite lines at  $\approx 20$ -25 eV (He I lines).

#### **4.4 Sketch of geometry and kinematics, outstanding questions**

From the dissimilar nature of the optical and far-UV spectrum (and the RV variations for SMC-SC4), we have been obliged to adopt a binary model involving nearly two equal mass A + B components. The strong double-peaked emission in the  $H_\alpha$  line against the continuum of an A bright giant or supergiant implies the presence of a flattened Keplerian disk.

The amplitude of the radial velocity variations compared to the almost stationary Balmer emission cores shows that at least in SMC-SC4 the  $H_\alpha$ -emitting structure is a circumbinary structure. We cannot rule out the possibility of RV variations in SMC-SC3 on the basis of their apparent consistency in just three observations. Indeed, the requirements to produce blueshifted He I line emission suggest unusual energetics in a region that has a different radial velocity than the A star. The orbital separation of the binary components, estimated above for SMC-SC4 to be  $\approx 1.7 \sin i^2$  AU, is about  $\frac{1}{3}$ - $\frac{1}{2}$  of the characteristic CB disk radius. The absence of forbidden emission or metastable absorption lines argues that most of the disk does not have a low density. The optical/IR colors imply that reddening from cool dust is negligible.

We envision that each of the binary component stars has a radiative wind, with the A star’s wind being weaker, slower, and perhaps denser near its surface.<sup>2</sup> These winds will interact along an annulus centered on the line connecting the two stars. The shock-heating in this wind will show a maximum intensity at velocities in between those of the stars, though not necessarily at the barycenter. This would explain the displacement of emission of the He I lines for SMC-SC3 and

<sup>2</sup> For ballpark numbers winds of early B stars may have  $\dot{M} \sim 10^{-9}$ - $10^{-8} M_\odot \text{ yr}^{-1}$  and a terminal velocity of 1000-2000  $\text{km s}^{-1}$ . Typical values for winds of A supergiants are thought to be  $\lesssim 10^{-7} M_\odot \text{ yr}^{-1}$  and 300  $\text{km s}^{-1}$  (e.g., Verdugo 2002).

Fe II lines for SMC-SC4. The wind continuously replenishes the CB disk, but we have no direct estimate of the relative amounts of disk or post-shock matter returning to the two stars or of it escaping through the outer edge of the CB disk. The symmetric emissions in the Fe II and other lines in the SMC-SC3 spectrum have a separate origin, and probably originate in the quasi-stationary CB disk.

Apart from the 1-2 BAC pattern in the spectrum of SMC-SC4, far wing absorptions appear in the opposite wing from far wing emissions (§3.6). Their juxtaposition suggests a common origin for these two non-BAC features. We suspect that their complex morphology arises from their formations along different sight lines to the A star and to flowing CS streams in the sky plane. This complicated behavior is reminiscent of red- and blueshifted components in time-resolved ultraviolet spectra in Algol systems. Peters & Polidan (1984, 1998) have noted the existence of flows associated with “High Temperature Accretion Regions” caused by streaming of wind efflux from the cool giant star as it expands and transits through the binary’s inner Lagrangian point. This stream collides with a disk around the receiving hot secondary. This is the reverse of the present context, in which the receiver is the cooler star. In the present case we envision that the collision points occur behind the orbiting primary and generate shocks. These are manifested in spectra as Doppler shifted emission components. Disk matter cools and eventually falls into the cool (A-type) star, rather than only through the inner Lagrangian point. The result is a complex array of relatively high velocity blue- and redshifted emission and absorption components that change their morphology around the orbital cycle. The high positive velocities compared to the A star in the 2009 spectrum (Fig. 11b, 12a) indeed suggests that matter falls toward the A star as seen from its trailing side, as Peters & Polidan found for the Algols. One aspect of this picture is that it predicts that the shock geometry can be complex and not necessarily repeatable from the cycle to cycle. Even at the same time the volumes producing emission for lines of different ions are not the same.

It is tempting to speculate that the infalling matter inferred from our 2009 spectra of SMC-SC4 is associated with the observed eclipses. Actually, any such picture must be complicated because it is the “wrong” (2007) spectrum which nearly coincides with the egress from a continuum light eclipse. This would suggest that the stream spirals nearly a complete circuit (some 65-90%) around the A star until it settles onto the star (the 2007 spectrum was obtained beyond the midpoint and during the egress of a photometric eclipse; see Table 1 here and Figure 6 in M10). Spectroscopically, this may be the cause of the second blueshifted absorption component of the strongest lines (e.g., dashed line in Fig. 2, solid line in Fig. 11b). At this binary phase the blue component might actually be a better measure of the A star’s velocity in orbit. The 2009 spectrum was taken at the

opposing phase, an infall phase in this picture, before the matter has piled up and settled to the surface. At this phase the light curve registers only a broad, small-amplitude depression. We note that our picture has some similarities with that presented by Soszynski (2007) to explain eclipses in interacting binary systems composed of red giants and low mass stars in the Large Magellanic Cloud.

## 5 SUMMARY AND CONCLUSIONS

Even as luminous variables in the SMC, our two program stars exhibit a extraordinary set of photometric and spectroscopic properties. These include a multiperiodic photometric variability, a  $\approx$ B3 type spectrum in the FUV, an optical A-type spectrum with Balmer emission lines and metallic lines from an intervening disk. For SMC-SC4 the spectral anomalies include the presence of one and sometimes two Discrete Blue Absorption Components (BACs) in metallic lines and RV variations. We have remarked that the optical spectrum of the SMC supergiant N82 in the SMC exhibits BACs and strong  $H_\alpha$  emission. However, unlike N82, neither of our stars shows forbidden lines. Because UV spectra are not available for N82, nor an optical RV campaign mounted, its suggested binary nature has not been tested.

We argue that our program stars reflect a comparatively brief stage in the life of intermediate mass  $\sim 9 M_\odot$  binary components. With separations of a few AU between the components, the winds of the two stars can interact and produce a large array of spectroscopic phenomenology. This phenomenology can include emissions in lines of intermediate and/or highly excited ions (e.g., He I) and time-variable pattern of sharp absorptions, in addition to the BACs. It is an open question why as many as two objects have such similarly unusual properties from a sample of only bright eight Mennickent Type 3 variables. In any case we may dub these objects prototypes of a presumably small group of Magellanic Cloud wind-interacting A + B binaries.

We speculate that the emission components originate from the interaction of that component of the A and B star winds in the zone near the line that intersects the centers of the two stars. The double peaked emissions in the Balmer lines disclose an emitting Keplerian disc, which from the peak separation has a larger extent than the binary separation. We have suggested, in part because of the He I line emissions in the SMC-SC3 spectrum, that wind-wind interactions cause localized heating and ionizing photons capable of exciting the observed level of  $H_\alpha$  model.

The Fe II line emission strengths are *anticorrelated* with the line's oscillator strengths. We have attributed this extraordinary circumstance to their formation in a geometrically thin but optically

thick and two layered column, where emission is formed in the deeper hotter shock and the absorption is just outside this region (though in the foreground of the observer's sight line). We have also speculated that wind-wind interactions in the zone between the stars collisionally excite He I line emission and also produce Balmer emission in the quasi-Keplerian circumbinary disc.

We have surmised that the primary BAC (absorption) feature is caused by the violent impact of the expanding A star wind into this CB disk. However, although we do not have enough observations to characterize the time-dependent secondary components well, it appears that the strengths of the emission components in either one of the far wings of the 3 eV Fe II lines are physically associated with absorptions in the opposite far wing.

We have speculated that a rich line profile variability, including the so-called secondary BACs and emission components, is a consequence of a matter stream originating from the wind of the B star and settling on the A star. This is a reverse Algol scenario in which matter is not constrained to flow only through the inner Lagrangian point. Perhaps this settling processes is responsible for the eclipses in the continuum light curve of SMC-SC4.

A number of observing programs can be suggested to test these ideas and conceivably offer new alternatives:

- A high-resolution monitoring of these objects should be undertaken to construct a radial velocity curve and determine the periods, separations, and inclinations of these systems. These same data can be used to trace the velocities of the various components in the primaries' spectra. For SMC-SC4 the features of interest are the BACs and the pairs of absorptions and emissions in the wings of the Fe II lines. For SMC-SC3 it is important to determine whether the velocity of the He I lines is constant or shows a small amplitude variation around the system's velocity.
- UV observations of the prominent resonance lines are needed to characterize the wind strength, velocity, and its behavior through the orbital cycle. We expect that these features are diagnostics of the B star's wind. It may also be possible to trace velocity changes in signatures of the A star's wind, such as an arguably Ca II K emission feature (Fig. 4b). In general, we expect the profiles of the UV resonance lines to be highly complex and variable.
- Any understanding of these particular objects rests on the expansion and adequate definition of this class, which in term entails finding more members. So far our small sample is drawn from a group of luminous optical/IR variables in the SMC. One prong of this search would be to find stars whose spectra exhibit BACs. To date we have obtained moderate resolution spectra of a number of luminous B stars in the OGLE surveys of both Clouds. We find that two LMC stars have properties

similar to our two prototype objects. These are OGLE05141821-6912350 and OGLE00552027-7237101. In addition, Mennickent et al. (2010) noted that the object OGLE LMC LPV-41682 ( $P = 219.9$  days; Soszynski 2010) exhibits modulated eclipses similar to those of SMC-SC4. Spectra of the two first objects display a range of  $H_\alpha$  emission profile intensities, strong absorptions among high level lines, and variable (possibly regular) light curves. Although the resolution of these spectra is sufficient to show at least strong forbidden emission lines, none are visible. If many of these stars are members of the group exemplified by SMC-SC3 and SMC-SC4, it will indicate that their properties are not isolated to a particular evolutionary age and/or angular momentum state. This is a possibility that we cannot yet dismiss.

## 6 ACKNOWLEDGMENTS

REM acknowledges support by Fondecyt grant 1070705, the Chilean Center for Astrophysics FONDAP 15010003 and from the BASAL Centro de Astrofísica y Tecnologías Afines (CATA) PFB-06/2007. We thank G. Pietrzyński and Dr. Darek Graczyk for his help with the OGLE database and observations. We thank Daniela Barría for her help with the reductions of LCO data. We also express our appreciation to Dr. D. J. Lennon for his suggestion that led to our working hypothesis of colliding winds in our program objects. Our FUSE work was supported by NASA Grant NNX07AC75G to the Catholic University of America.

## REFERENCES

- Bagnulo S., Jehin E., Ledoux C., Cabanac R., Melo C., Gilmozzi R., The ESO Paranal Science Operations Team, 2003, *Msngr*, 114, 10; <http://www.sc.eso.org/santiago/uvespop/>
- Blair, W. P., Oliveira, C., et al. 2009, *PASP*, 121, 634
- Dixon, W. V., Sahnou, D. J., Kruk, J. W., et al. 2007, *PASP*, 119, 527
- Dolphin A. E., Walker A. R., Hodge P. W., Mateo M., Olszewski E. W., Schommer R. A., Suntzeff N. B., 2001, *ApJ*, 562, 303
- Dufton P. L., Ryans R. S. I., Trundle C., Lennon D. J., Hubeny I., Lanz T., Allende Prieto C., 2005, *A&A*, 434, 1125
- Evans, C. J., Lennon D. J., Smartt, S. J., Trundle, C. 2006, *A&A*, 456, 623E
- Heydari-Malayeri, M. 1990, *A & A*, 234, 233
- Hubeny, I & Heap, S. R. 1996, *ApJ*, 470, 1144

- Hubeny, I., Lanz, T., & Jeffery, C. S. 1994, *Newsl. Anal. Astron.*, 20, 30
- Jaschek, M., Jaschek, C., & Andrillat, Y. 1988, *A&AS*, 72, 505
- Kurucz, R. L. 1993, Kurucz CD-Rom #13
- Martayan, C., Baade, D., & Fabregat, J. 2010, *A&A*, 509, A11
- Mennickent, R. E., Pietrzyński, G., Gieren, W., et al. 2002, *A&A*, 393, 887
- Mennickent, R. E., Cidale, L., Pietrzyński, G., et al. 2006, *A&A*, 457, 949 (M06)
- Mennickent R. E., Kołaczowski Z., Michalska G., Pietrzyński G., Gallardo R., Cidale L., Granada A., Gieren W., 2008, *MNRAS*, 389, 1605
- Mennickent, R. E., Smith, M. A., Kołaczowski, Z., Pietrzyński, G., Soszyński, I. 2010, *PASP*, xx, xxx; arXiv:1004.2728 (M10)
- Mighell K. J., Sarajedini A., French R. S., 1998, *ApJ*, 494, L189
- Pellerin, A., Fullerton, A. W., Robert, C., et al. *ApJSS*, 143, 159
- Peters, G. J. & Polidan, R. S. 1984, *ApJ*, 283, 745
- Peters, G. J. & Polidan, R. S. 1998, *ApJ*, 500, L17
- Schiller, F., & Przybilla, N. 2008, *A&A*, 479, 849
- Skiff, B. A. 2009 VizieR on line catalog: “Catalog of Stellar Spectral Classifications”
- Smith, M. A. 2010, *ApJS*, 186, 175
- Soszynski, I. 2007, *ApJ*, 660, 1486
- Soszynski, I. 2010, priv. comm.
- Udalski A., Kubiak M., Szymański M., 1997, *AcA*, 47, 319
- Verdugo, E., Talavera, A., & Gomez de Castro, A. I. 1999, *A&A*, 346, 819
- Verdugo, E., Gomez de Castro, A., Ferro-Fontan, C., et al. 2002, *ASPC*, 259, 574
- Verdugo, E., Henrichs, H. F., Talavera, A., et al. 2005, *ASPC*, 337, 324